Int. J. Electrochem. Sci., 7 **(2012)** 5400 - 5419

International Journal of ELECTROCHEMICAL SCIENCE
www.electrochemsci.org

Temperature and Time Investigations on the Adsorption Behavior of Isoindoline, Tetrazole and Isoindoline-Tetrazole on Corrosion of Mild Steel in Acidic Medium

Y. Aouine[1], *M. Sfaira*[2*], *M. Ebn Touhami*[3], *A. Alami*[1], *B. Hammouti*[4], *M. Elbakri*[3], *A. El Hallaoui*[1], *R. Touir*[3]

[1] Laboratory of Organic Chemistry, Faculty of Sciences Dhar El Mahraz, Sidi Mohammed Ben Abdellah University, BP 1796 – 30000, Atlas – Fez, Morocco.
[2] Laboratory of Materials Engineering, Modelling and Environment, Faculty of Sciences Dhar El Mahraz, Sidi Mohammed Ben Abdellah University, BP 1796 – 30000, Atlas – Fez, Morocco.
[3] Laboratory of Materials, Electrochemistry and Environment, Faculty of Sciences, University Ibn Tofail, BP. 133 – 14000, Kénitra, Morocco.
[4]:LCAE-URAC18, Faculty of Sciences, Mohammed the 1st University, BP 717 – 60000, Oujda, Morocco.
[*]E-mail: msfaira@yahoo.com

Received: 23 February 2012 / *Accepted:* 27 April 2012 / *Published:* 1 June 2012

The inhibition effect of new three heterocyclic compounds, namely (2-(1,3-dioxoisoindolin-2-yl) acetonitrile (*IND*), 2-((1H-tetrazol-5-yl) methyl) isoindoline-1,3-dione (*IND-TET*) and 5-(chloromethyl)-1H-tetrazole (*TET*)) on mild steel corrosion in molar hydrochloric acid (1 M HCl) has been investigated. It was studied through polarization and electrochemical impedance spectroscopy techniques. The inhibiting efficiency was found to depend on both concentration and immersion time and circa temperature-independent. *IND* and *IND-TET* were of cathodic type wile *TET* was mixed type influencing predominately cathodic process. From the temperature dependences, the activation energy in the presence of inhibitors found to be inferior to that in uninhibited medium. The adsorption of the inhibitors was well described by the Langmuir adsorption isotherm model. The influence of molecular structure was discussed and no synergism was observed in the case of *IND-TET* inhibitor.

Keywords: Corrosion, Inhibition, Mild Steel, molar HCl, isoindoline and tetrazole derivatives

1. INTRODUCTION

Mild steel is extensively used in many industrial applications and gets corroded when exposed to different industrial environment. Acidic solutions are widely used in industry, i.e.; acid pickling,

acid cleaning, acid descaling and oil-aciddizing, etc. [1]. Many chemical substances are used to protect metals against corrosion. The application of inhibitors to prevent corrosion of metals is an extremely important area. These compounds can adsorb on the metal surface and block the active sites and thereby slow down the corrosion rate. The mechanism action of inhibitors is of great importance and depends on the formulation as well as rational use in various environments. The electronic characteristic of the adsorbate molecules, the solution chemical composition, the nature of metallic surface, the temperature of the reaction, the immersion time and the electrochemical potential at the metal–solution interface determine the adsorption degree and hence the inhibition efficiency [2].

The corrosion inhibitors of mild steel are generally heterocyclic compounds containing nitrogen, sulphur and/or oxygen atoms. Moreover, many N-heterocyclic compounds have been proved to be effective inhibitors in hydrochloric acid. Indeed, several triazoles [3,4], pyrazoles [5], imidazoles [6-8], pyridazines [9,10]…etc, have been among the best known and the most studied inhibitors. Notwithstanding several structural similarities with some of the above mentioned compounds, the tetrazole [11-13] and indoline [14] derivatives have been scarcely studied as mild steel corrosion inhibitors.

The aim of the present work is to study the inhibition properties of 2-(1,3-dioxoisoindolin-2-yl) acetonitrile, 2-((1H-tetrazol-5-yl) methyl) isoindoline-1,3-dione and 5-(chloromethyl)-1H-tetrazole, denoted hereafter (*IND*), (*IND-TET*), and (*TET*), respectively on the mild steel corrosion in molar hydrochloric acid. It is also aimed to predict the thermodynamic feasibility of inhibitors adsorption on metallic surface. To this end, potentiodynamic polarization curves, Tafel plot analysis and electrochemical impedance spectroscopy (EIS) were the corrosion test used in this study. Beside detailed investigation of temperature and immersion time effects on the system's electrochemical parameters was also studied and discussed to more understanding the adsorption mechanism of the studied inhibitors.

2. EXPERIMENTAL DETAILS

2.1.Material preparation

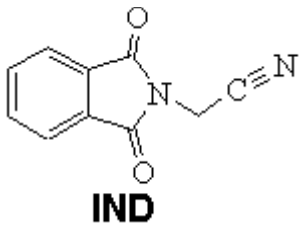

2-(1,3-dioxoisoindolin-2-yl)acetonitrile

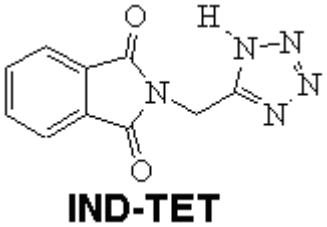

2-((1H-tetrazol-5-yl)methyl)isoindoline-1,3-dione

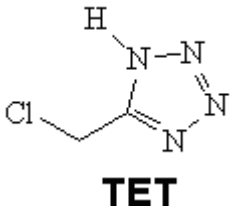

5-(chloromethyl)-1H-tetrazole

Figure 1. Name and chemical structures of the investigated organic compounds

The structural formulas of the inhibitors examined in this study are shown in Fig. 1. Corrosion tests were performed on a mild steel of following percentage composition 0.09% P; 0.38% Si; 0.01% Al; 0.05% Mn; 0.21% C; 0.05% S and remainder iron. The surface of specimens was carried out by grinding with emery paper of different grit sizes (from 180 to 1200), rinsing with doubly distilled water, degreasing in ethanol, and drying before use. The aggressive solution of 1 M HCl was prepared by dilution of analytical grade 37% HCl with doubly distilled water.

2.2. Electrochemical measurements

For electrochemical measurements, a conventional three-electrode glass cell with a platinum counter electrode and a saturated calomel electrode (SCE) as reference was used. Mild steel cylindrical rod of the same composition as working electrode was pressure fitted into a polytetrafluoroethylene holder (PTFE) to avoid any infiltration of electrolyte then exposing only 1 cm^2 surface to the aggressive solution. The test solution was thermostatically controlled at 25 °C in air atmosphere without bubbling. All potentials were measured against SCE.

The polarization curves were recorded by changing the electrode potential automatically with a Potentiostat/Galvanostat type PGZ 100, at a scan rate of 1 mV s^{-1}. Before each experiment, the working electrode was immersed in the test cell for an hour until reaching steady state.

The data in Tafel region have been processed for evaluation corrosion kinetic parameters by plotting the polarization curves. The linear Tafel segments, in a large domain of potential, of the cathodic curves were extrapolated to the corresponding corrosion potentials to obtain the corrosion current values. The inhibition efficiency was evaluated using the relationship (1):

$$IE_{I-E} = \frac{i_{corr}^{0} - i_{corr}}{i_{corr}^{0}} \times 100 \quad (1)$$

i_{corr}^{0} and i_{corr} are the corrosion current densities values without and with inhibitors, respectively.

The current-potential plots recorded, in the vicinity of the free corrosion potential E_{corr}, give the corresponding polarisation resistance, R_P, of mild steel in 1 M HCl in the presence of various concentrations of the studied inhibitors. The corresponding inhibition efficiency was derived from the relationship (2):

$$IE_{R_P}\,\% = \frac{R_P - R_P^{'}}{R_P} \times 100 \quad (2)$$

R_P and R'_P are the polarisation resistances with and without the studied inhibitors, respectively.

The values of the degree of surface coverage (θ) have been obtained from polarization curves for various concentrations of inhibitors. Here, θ can be given as (3) [15]:

$$\theta = 1 - \frac{i_{corr}}{i_{corr}^{0}} \quad (3)$$

The electrochemical impedance spectroscopy measurements were carried out using a transfer function analyzer (VoltaLab PGZ 100), with a small amplitude ac. signal (10 mV rms), over a frequency domain from 100 kHz to 10 mHz at 25 °C on air atmosphere with 5 points per decade. Computer programs automatically controlled the measurements performed at rest potentials after 1 h of immersion at E_{corr}. The impedance diagrams were given in the Nyquist representation. To determine the impedance parameters of the mild steel specimens in acidic solution, the measured impedance data were analyzed using Bouckamp program based upon an electric equivalent circuit [16]. The inhibition efficiency of the inhibitors has been determined from the relationship (4):

$$IE_{imp}\% = \frac{R_t - R_t^0}{R_t} \times 100 \quad (4)$$

R_t^0 and R_t are the charge transfer resistance values in the absence and in the presence of inhibitors, respectively.

3. RESULTS AND DISCUSSION

3.1. Tafel extrapolation

Polarization measurements have been carried out in order to gain knowledge concerning the kinetics of the anodic and cathodic reactions. Potentiodynamic curves are obtained in the presence and absence of the studied inhibitors, after pre-polarizing the electrode at its E_{corr} for one hour, thereafter pre-polarized at -800 mV for 10 min. After this scan, the potential was swept stepwise from the most cathodic potential to the anodic direction.

Table 1. Values of electrochemical parameters evaluated from the cathodic current-voltage characteristics for the system electrode/1 M HCl with and without added inhibitors at 298 K

Inhibitor	Concentration mol L^{-1}	E_{corr} mV_{sce}	$\lvert \beta_c \rvert$ mV dec^{-1}	i_{corr} µA cm^{-2}	R_P Ω cm^2	EI_{Rp} %	EI_{I-E} %
Blank	0	-432	156	470	40	-	-
IND	10^{-4}	-443	112	97	220	82	79
	$5\ 10^{-4}$	-449	142	88	242	83	81
	10^{-3}	-444	131	79	266	85	83
IND-TET	$5\ 10^{-5}$	-466	123	103	115	65	78
	10^{-4}	-474	115	86	231	83	81
	$5\ 10^{-4}$	-479	105	36	323	88	92
	10^{-3}	-484	102	31	497	92	93
TET	$5\ 10^{-4}$	-401	117	104	120	67	78
	10^{-3}	-386	80	34	416	90	93

This avoided electrolyte pollution by dissolved iron. The current-potential plots recorded in the vicinity of E_{corr} (not shown here) give the corresponding polarisation resistance, R_P, of mild steel in 1 M HCl in the presence of various concentrations of the studied inhibitors.

The effect of rise concentration of *IND*, *IND-TET* and *TET* on the anodic and cathodic polarisation curves of mild steel in 1 M HCl at 298 K is presented in Fig. 2. Various corrosion parameters such as corrosion current densities (i_{corr}), corrosion potentials (E_{corr}), cathodic Tafel slopes (β_c), degree of surfaces coverage (θ) and inhibition efficiencies $IE_{I\text{-}E}\%$, $IE_{Rp}\%$ obtained from polarization measurements are listed in Table 1.

From the recorded results, we can conclude that in all cases, addition of the studied compounds induced a marked decrease in the cathodic and a slight decrease in the anodic current densities. Accordingly, these inhibitors affect greatly the hydrogen reaction discharge and slightly affect the mild steel dissolution processes. The hydrogen evolution reaction is under activation control since the cathodic portions rise to Tafel lines. The fact that cathodic process slow down can be due to the covering of the surface with monolayer of the tested molecules due to the adsorbed inhibitors on the mild steel surface then reducing the electrolyte infiltration to the interface. This idea is investigated in separate section by plotting of suitable adsorption isotherm.

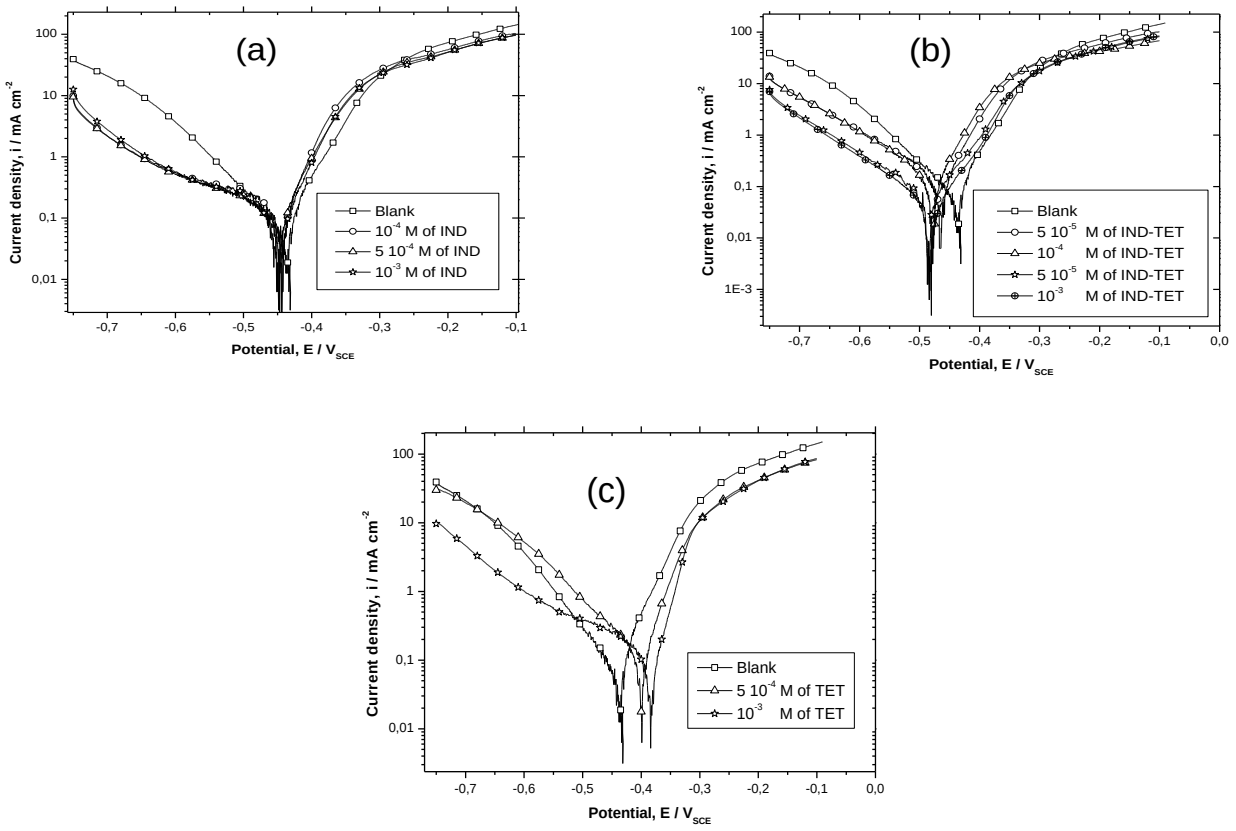

Figure 2. Potentiodynamic polarization curves obtained for mild steel at 298 K in 1 M HCl at various concentrations of the studied inhibitors (a): *IND*, (b): *IND-TET* and (c) *TET*

It can be seen from Table 1, that E_{corr} values show significant shift cathodically at various concentrations of *IND* and *IND-TET*, suggesting that *IND* and *IND-TET* are mainly cathodic-type inhibitors in 1 M HCl. In contrast, E_{corr} trends towards more anodic direction in the case of *TET* with a both decrease in the anodic and cathodic branches. *TET* seems to be mixed-type inhibitor with marked cathodic behavior. Cathodic Tafel slopes β_c, were approximately constant, meaning that the inhibiting action of these molecules occurred by simple blocking of the available surface area; i.e. the inhibitors decreased the surface area for hydrogen evolution without affecting the reaction mechanism [17].

From Table 1, it can be seen that i_{corr} values decreased substantially with increasing inhibitors concentration and reached a minimum at 10^{-3} M whereas $IE_{I\text{-}E}\%$ increases with inhibitors concentration. Indeed, the corrosion current density value decreases from 470 µA cm^{-2} in uninhibited medium to 79, 31 and 34 µA cm^{-2} in presence of 10^{-3} M for *IND*, *IND-TET* and *TET*, respectively resulting in the efficiency of 83%, 93% and 93%. The inhibition efficiency $IE_{I\text{-}E}\%$ of these compounds follows the sequence $TET \approx IND - TET > IND$ for the various concentrations used; this behavior can be attributed to the presence of electron donating groups (oxygen, nitrogen, aromatic ring) in *TET* and *IND-TET* compounds. The presence of free electron pairs in nitrogen atoms and π-electrons on aromatic rings favors the adsorption of *TET* and *IND-TET* on mild steel surface. Similar results have been recorded with other tetrazole derivatives [18] on Al surface. These results revealed the strong inhibiting effect of the studied inhibitors. It is to be noted that no synergism is observed in *IND-TET* molecule compared to *IND* and *TET* taken separately and the performance of *IND-TET* can be attributed only to the presence of tetrazolic ring in this last molecule.

The order of the increase of $IE_{Rp}\%$ (Table 1), derived from polarization resistance R_p determined from the slope of polarization curves, with respect to the change in the molecular structure was similar to the results obtained from the Tafel extrapolation.

3.2. Electrochemical impedance spectroscopy (EIS) study

Impedance measurements provide information on both the resistive and capacitive behavior of the interface and makes possible to evaluate the performance of the studied inhibitors. Before each EIS experiments, as done with Tafel experiments, the electrode was allowed to corrode freely for an hour to obtain a steady-state open circuit potential, corresponding to the corrosion potential, E_{corr}, of the working electrode.

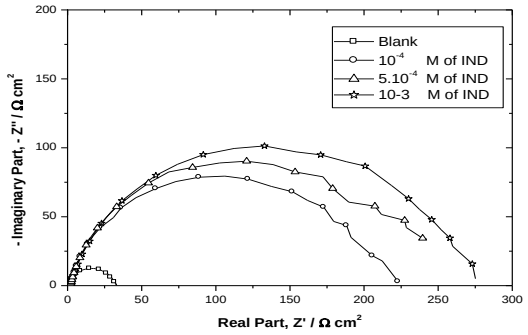

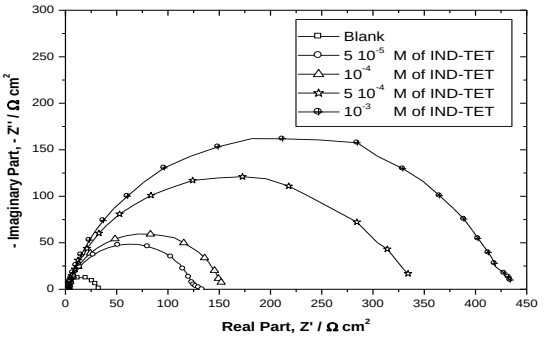

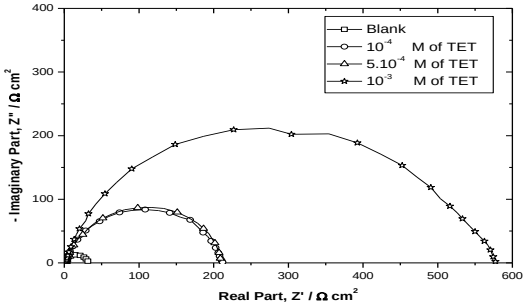

Figure 3. Nyquist plots for mild steel at 298 K in 1 M HCl in various concentrations of the studied inhibitors (a): *IND,* (b): *IND-TET* and (c) *TET*

The influence of the different investigated organic compounds and their concentration on the corrosion of mild steel in 1 M HCl by EIS are shown in Fig. 3. The impedance behavior of mild steel corrosion, in the form of Nyquist plots, exhibits one semicircle, which centre lies under the abscissa. These diagrams have similar shape; the shape is maintained throughout all tested concentrations, indicating that almost no change in the corrosion mechanism occurred due to the inhibitors addition. This behavior can be attributed to charge transfer of the corrosion process and the diameter of semicircle increases with increasing inhibitors concentration.

The transfer function can be represented by a resistance R_1 parallel to a capacitor C and in series to them an additional resistance R_2 as expressed in equation (5):

$$Z(\omega) = R_2 + (\frac{1}{R_1} + j\omega C)^{-1} \qquad (5)$$

This transfer function is applicable for homogeneous systems with one time constant when the centre of the semicircle lies on the abscissa of real part. It is evident that it cannot describe the observed depression of the capacitive loop and it is necessary to replace the capacitor by some element taking into account frequency dispersion like the Constant Phase Element (*CPE*). This element is a generalised tool, which can reflect exponential distribution of the parameters of the electrochemical reaction related to energetic barrier at charge and mass transfer.

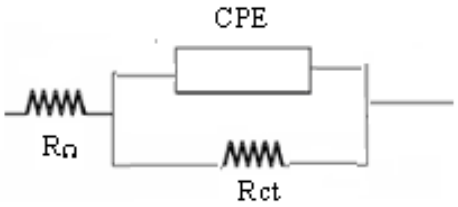

Figure 4. Suggested equivalent circuit model of the interface mild steel/1 M HCl with and without the studied inhibitors

Such phenomena often correspond to surface heterogeneity which may be the result of surface roughness, dislocations, distribution of the active sites or adsorption of inhibitors [19]. In order to fit and analyze the EIS data, the equivalent circuit shown in Fig. 4 is selected.

This circuit is generally used to describe the iron/acid interface model [20]. In this equivalent circuit, R_{ct} reflects the charge transfer resistance R_1, R_Ω is the resistance of the solution R_2, and *CPE* is a constant phase element which replace the pure capacitor. The impedance function of the *CPE* is as follows (6):

$$Z_{CPE} = Y^{-1}(j\omega)^{-n} \quad (6)$$

Y is the magnitude of *CPE* and *n* an exponent related to the phase shift, both of them are frequency independent, and ω is the angular frequency. For whole numbers of *n* = 1, 0, -1, *CPE* is reduced to the classical lumped elements capacitor (*C*), resistance (*R*) and inductance (*L*), respectively. The value of *n* = 0.5 corresponds to Warburg impedance (W). Other values of *n* approximately describe other types of frequency distribution behavior of *C*, *R*, *L* or *W* with distributed parameters [21]. In real iron/acid interface systems, ideal capacitive behavior is not observed due to roughness, or uneven current distributions on the electrode surface which results in frequency dispersion [22,23]; therefore a *CPE* is usually used instead of a capacitance C_{dl} (double layer capacitance) to fit more accurately the impedance behavior of the electrical double layer. The idealized capacitance (C_{id}) values can be described by *CPE* parameter values *Y* and *n* using the following expression (7) [24]:

$$C_{id} = \frac{Y\omega^{n-1}}{\sin(n\pi/2)} \quad (7)$$

Table 2. EIS data of mild steel in 1 M HCl containing different concentrations of the studied inhibitors at 298 K

Inhibitor	Concentration mol L^{-1}	R_{ct} Ω cm^2	C_{dl} μF cm^{-2}	IE_{imp} %	θ
Blank	0	32	160	-	-
IND	10^{-4}	222	52	85	0.856
	$5\ 10^{-4}$	255	47	87	0.874
	10^{-3}	276	21	88	0.884
IND-TET	$5\ 10^{-5}$	130	43	75	0.754
	10^{-4}	152	35	79	0.789
	$5\ 10^{-4}$	335	18	90	0.904
	10^{-3}	434	16	93	0.926
TET	10^{-4}	209	30	84	0.847
	$5\ 10^{-4}$	212	27	85	0.849
	10^{-3}	576	16	94	0.944

Table 2 shows that R_{ct} values increased with increasing inhibitors concentration and the results indicated that charge transfer process mainly controls the corrosion process. The decrease in C_{dl} values with increasing inhibitors concentration indicating that inhibitors function by adsorption at the metal/solution interface by gradual displacement of water molecules originally and/or chloride ions on the mild steel surface [25] leading to a protective solid film, inhibiting species or both on the mild steel surface, then decreasing the extend of dissolution reaction [26, 27]. The corresponding inhibiting efficiencies $IE_{imp}\%$ values indicate that by the increase of inhibitors concentration, their values increase too. The inhibition efficiencies, got from electrochemical impedance measurements, show the same trend as those obtained from polarization measurements.

The thickness of the protective layer (d) increases with rise inhibitors concentration, since more *IND*, *TET* and *IND-TET* will electrostatically adsorb on the electrode surface, resulting in a noticeable decrease in C_{dl}. This trend is in accordance with Helmholtz model, given by the following equation (8) [28]:

$$C_{dl} = \frac{\varepsilon \varepsilon_0 S}{d} \quad (8)$$

ε is the dielectric constant of the protective layer, ε_0 is the permittivity of free space ($8.854\ 10^{-14}$ F cm^{-1}) and S is the effective surface area of the electrode.

Two modes of adsorption can be considered. The process of physical adsorption requires the presence of electrically charged metal surface and the charged species in the bulk of the solution. Chemisorption process involves charge sharing of charge transfer from the inhibitor molecules to the metal surface. This is possible in case of positive as well as negative charges on the surface. The presence of a transition metal, having vacant, low-energy electron orbital, and an inhibitor molecule having relatively loosed bound electrons or heteroatoms with lone-pair electrons facilitates this adsorption [29]. On the other hand, *IND*, *TET* and *IND-TET* which possess nitrogen and oxygen atoms and lone-pair electrons, can accept a proton, leading the cationic forms. These species can adsorb on the metal surface because of attractive forces between the negatively charged metal and the positively inhibitors.

3.3. Thermodynamic parameters of the adsorption process

The adsorption isotherm can be determined if the inhibitor effect is due mainly to the adsorption on metallic surface (i.e. to its blocking). The adsorption isotherm type can provide additional information about the tested compounds properties. The fractional coverage surface (θ) can be easily determined from ac impedance, Tafel polarization or the linear polarization by the ratio *IE%/100*. In the present study, the inhibiting efficiency is evaluated from impedance measurements. If one assumes that the values of $IE_{imp}\%$ do no differ substantially from θ as shown in Table 2. The adsorption isotherms models considered were as described in reference [43]:

Temkin isotherm $\exp(f.\theta) = K_{ads}\, C_{inh}$ (9)

Langmuir isotherm $$\frac{\theta}{1-\theta} = K_{ads} C_{inh} \quad (10)$$

Frumkin isotherm $$\frac{\theta}{1-\theta} \exp(-2f\theta) = K_{ads} C_{inh} \quad (11)$$

Freundluich isotherm $$\theta = K_{ads}\, C_{inh} \quad (12)$$

Where K_{ads} is the equilibrium constant of the adsorption process, C_{inh} is the inhibitor concentration and f is the factor of energetic inhomogeneity. The linear coefficient regression, r was used to choose the isotherm that best fit experimental data (Table 3).

Table 3. Equilibrium constant and free energy of adsorption values for 1 h in presence of the studied inhibitors in 1 M HCl on mild steel

Inhibitor	Slope	K_{ads} L mol^{-1}	$\Delta_{ads}G°$ kJ mol^{-1}	Linear coefficient regression (r)
IND	1.12	17.334 10^4	- 39.84	0.9999
IND-TET	1.06	5.704 10^4	- 37.09	0.9999
TET	1.04	3.002 10^4	- 35.49	0.9917

The best fitted straight line (strong correlation with r>0.99) is obtained for the plot of C_{inh}/θ vs. C_{inh} with slopes around unity. This suggests that the adsorption of the studied inhibitors on metallic surface obeyed to the Langmuir's adsorption isotherm model (Fig. 5).

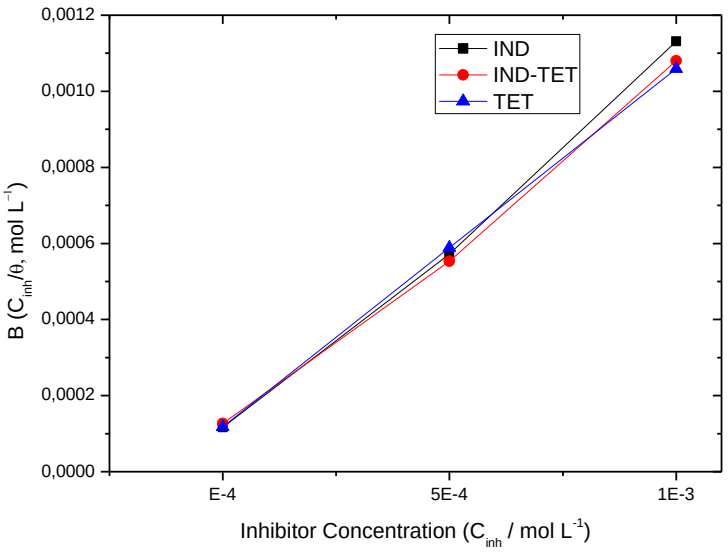

Figure 5. Langmuir adsorption isotherm plot for mild steel in 1 M HCl at different concentrations of the studied inhibitors

From the intercepts of the straight lines C_{inh}/θ vs. C_{inh}, K_{ads} value can be calculated. The constant of adsorption, K_{ads}, is related to the standard free energy of adsorption, $\Delta_{ads}G^0$, by the following equation (13) [30]:

$$K_{ads} = \frac{1}{55{,}55}\exp\left(-\frac{\Delta_{ads}G^{\circ}}{RT}\right) \quad (13)$$

55.55 represent the concentration of water in solution in mol L^{-1}, R is the universal gas constant and T is the absolute temperature. The standard free energy of adsorption, $\Delta_{ads}G^0$ can be calculated. The negative values of $\Delta_{ads}G^0$ ensure the spontaneity of the adsorption process and stability of the adsorbed layer on mild steel surface. It is well known that values of $\Delta_{ads}G^0$ of order of 20 kJ mol^{-1} or lower indicate a physisorption; while those of order of 40 kJ mol^{-1} higher are associated with chemisorption [31]. Values of $\Delta_{ads}G^0$ are as reported in Table 3 - 39.84, - 37.09 and - 35.49 kJ mol^{-1} for *IND*, *IND-TET* and *TET*, respectively. It is suggested that the adsorption mechanism of the investigated inhibitors on the mild steel surface in 1 M HCl solution involves two types of interaction; chemisorption and physisorption [4].

Hence it can be suggested that each inhibitors adsorb on metallic surface forming strong chemisorption bonds. This is in fact possible in view of the presence of unshared electron pairs in the organic compounds molecules and taking into consideration the behaviour of Fe as electrons acceptor as its d-submonolayer is incomplete. The inhibitors studied may then be adsorbed via donor–acceptor interactions between the π-electrons of the aromatic systems and the unshared electrons pairs of the heteroatoms (-N, -O) to form a bond with the vacant d orbital of the iron atom on the metal surface, which act as a Lewis acid, leading to the formation of a protective chemisorbed film.

Beside the fact that the inhibition phenomenon can be imputed to the presence of empty d-orbital in the Fe which led to an easier coordinate bond formation between the metal and inhibitors, these last contain nitrogen and oxygen atoms which are easily protonated in HCl medium. Therefore, physical adsorption is also possible via electrostatic interaction between a negatively charged surface, which is provided with a specifically adsorbed chloride anion on mild steel, and the positive charge of the inhibitors [32].

3.4. Thermodynamic parameters of the activation corrosion process

In order to gain more information about the type of adsorption and the effectiveness of the investigated inhibitors at higher temperatures, potentiodynamic polarization measurements (Fig. 6) were carried out at different temperatures (25–55°C) for mild steel electrode in 1 M HCl without and with inhibitors after an hour of hold time immersion in free corrosion potential. The corresponding data derived from these Figures (6a-d) are collected in Table 4. Increasing the solution temperature leads to increasing the current density values of the two branches of the polarization curves and consequently the values of i_{corr}. However, the increase in current density is highly more pronounced in uninhibited than in inhibited media. Indeed, it is worth noting that the values of i_{corr} in the presence of

inhibitors are always weaker than its values in the absence of inhibitors and the differences between its values in absence and presence of the inhibitors increase with temperature.

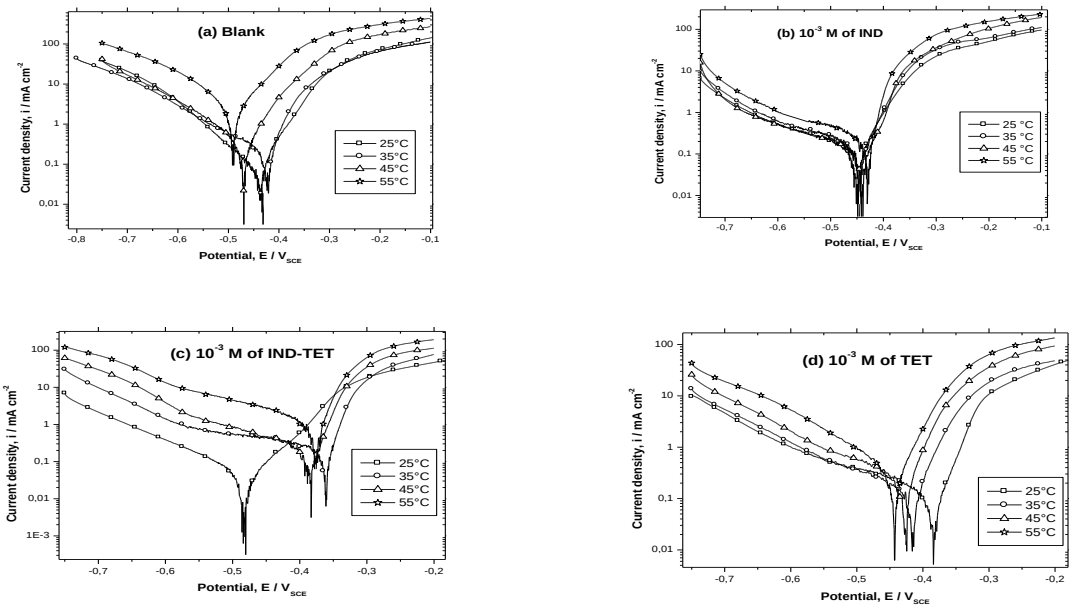

Figure 6. Effect of temperature on the behaviour of mild steel / 1 M HCl interface in (a) uninhibited solution, (b) at 10^{-3} M of *IND*, (c) at 10^{-3} M of *IND-TET* and (d) at 10^{-3} M of *TET*

Table 4. Electrochemical characteristics of mild steel in 1 M HCl with and without 10^{-3} M of the studied inhibitors at different temperatures derived from current-voltage *I-E* characteristics

Inhibitor	Temperature K	E_{corr} mV_{sce}	i_{corr} $\mu A\ cm^{-2}$	IE_{I-E} %	θ '
Blank	298	-432	470	-	-
	308	-422	774	-	-
	318	-471	1540	-	-
	328	-429	3863	-	-
IND	298	-444	79	83	0.832
	308	-446	143	82	0.815
	318	-439	292	81	0.810
	328	-430	593	84	0.844
IND-TET	298	-484	37	92	0.921
	308	-362	101	87	0.869
	318	-384	138	91	0.910
	328	-377	316	92	0.918
TET	298	-386	34	93	0.927
	308	-416	48	94	0.938
	318	-428	69	96	0.955
	328	-443	102	97	0.974

Moreover, no clear trends are observed in E_{corr} values at higher temperatures in free medium and with *IND* as well as *IND-TET* whereas, cathodic shifts is registered in the presence of *TET*. These results reflect the enhancement of both the cathodic hydrogen evolution reaction as well as anodic mild steel dissolution with the rise of temperature. However, the values of $IE_{I\text{-}E}$, calculated from i_{corr} according to equation (1) and consequently the degree of surface coverage θ' ($\theta' = IE_{I\text{-}E}/100$) remain almost constant in the case of *IND* and *IND-TET* whereas a slight increase in noticed in the presence of *TET*. This behavior, together with the higher adsorption equilibrium constant K_{ads} values of Table 3 confirms the chemisorption of the studied inhibitors on the mild steel surface. As reported elsewhere [33], the fact that the $IE_{I\text{-}E}\%$ increases with temperature is explained by some authors as likely specific interaction between the iron surface and the inhibitor. Ivanov [34] explains this increase with temperature by the change in the nature of the adsorption mode; the inhibitor is being physically adsorbed at lower temperatures, while chemisorption is favored by increasing of temperature. The same phenomenon is explained by others coworkers [35] as an increase in the surface coverage by the inhibitor. Thus, at a high degree of coverage, the diffusion through the surface layer containing the inhibitor and corrosion products becomes the rate-determining step of the metal dissolution process [14]. These results broaden the use of our investigated inhibitors in many applications in which the solution temperature is raised during proceeding, e. g. cooling water systems.

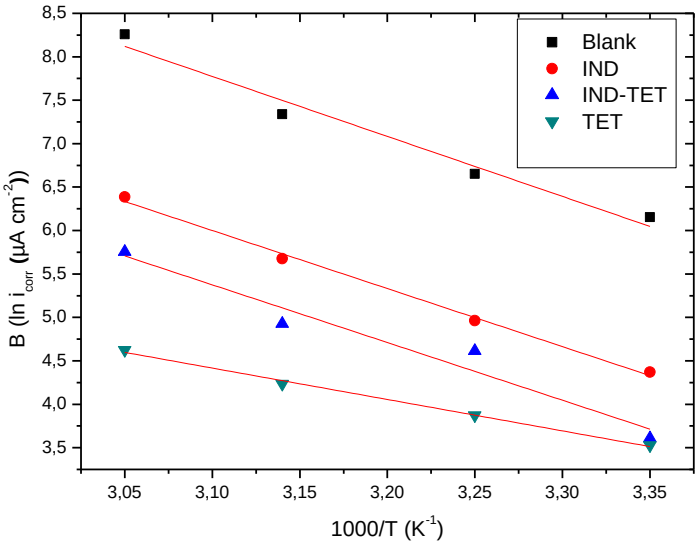

Figure 7. Arrhenius plots of mild steel in 1 M HCl with and without 10^{-3} M of the studied inhibitors

Figure 7 illustrates the dependence of the corrosion rate in Arrhenius coordinates in presence and absence of inhibitors determined at the highest concentration used, in order to assure that the achieved coverage degree is close to the maximal value; i.e. the concentration which gives the best inhibiting efficiency. The corrosion process can be regarded as an Arrhenius type process, the rate of which is given by equation (14):

$$\ln i_{corr} = \ln A - \frac{E_a}{RT} \quad (14)$$

Where E_a is the apparent activation energy of corrosion process, R is the universal gas constant, A is the Arrhenius pre-exponential constant and T is the absolute temperature.Values of E_a for mild steel in 1 M HCl in the absence and the presence of each inhibitors were determined from the slope of *ln* i_{corr} vs. *1/T* plots and shown in Table 5 which include as well the pre-exponential term, *A*. All the linear regression coefficients between *ln* i_{corr} vs. *1/T* are very close to 1, which indicates that the linear relationship considered is very good.

Table 5. The values of activation parameters E_a, $\Delta_a H^*$ and $\Delta_a S^*$ for mild steel in 1 M HCl and added of 10^{-3} M of the studied inhibitors

Inhibitor	Pre-exponential factor, *A* μA cm^{-2}	E_a kJ mol^{-1}	$\Delta_a H^*$ kJ mol^{-1}	$\Delta_a S^*$ J K^{-1} mol^{-1}
Blank	4.74 10^{12}	57.43	54.33	-31.64
IND	0.40 10^{12}	55.56	50.89	-57.36
IND-TET	0.02 10^{12}	55.24	52.59	-56.94
TET	6.09 10^{6}	30.05	27.22	-143.61

According to equation (14), it can be seen that the lower *A* and the higher E_a values, the lower is the current density i_{corr}. For the present study, the values of *A* as well as E_a in the presence of inhibitors follow the same trend and are lower than those in uninhibited solution. So the decrease in mild steel corrosion rate is determined by the pre-exponential factor.

The E_a value corresponds to that of hydrogen ions activation and in fact can be considered as a verification of the cathodic control of the corrosion process in 1 M HCl [14,36]. Hence, the temperature increase will lead to a decrease of hydrogen evolution overvoltage. The values of E_a found for *IND*, *IND-TET* are close, but still lower than in 1 M HCl whereas for *TET*, E_a drops down and is circa the half compared to the blank solution. They increase in the same order as the ranking of the inhibitors; i.e. E_a *(TET)* < E_a *(IND-TET)* < E_a *(TET).*

It is well recognized that the temperature dependence of the inhibition effect and the comparison of the values of the apparent activation energy, E_a, of the corrosion process in absence and presence of inhibitors can provide further evidence [37,38] concerning the mechanism of the inhibition action. The decrease of the inhibitor efficiency with increasing temperature, which refers to a higher value of E_a, when compared to free solution, is interpreted as an indication for an electrostatic character of the inhibitor's adsorption. However, the lower value of E_a in inhibited solution compared to uninhibited solution can be explained by strong chemisorption bond between the inhibitor and the metal. Some authors reported that electrostatic adsorption proceeds irrespective of the fact that the E_a value in the presence of inhibitor is lower than that in free solution [39].

Hence, the addition of the studied inhibitors affects the values of E_a; this modification maybe attributed to the change in the corrosion process mechanism in the presence of adsorbed inhibitor

molecules [40]. The lower values of the activation energy of the corrosion process in the presence of inhibitors compared to free solution is attributed to their chemisorption, while the opposite is generally attributed to the physical adsorption [37]. Then, it can be suggested that *IND*, *IND-TET* and *TET* adsorb on the mild steel surface forming strong chemisorption bonds. It is well known that the chemisorption process is charge sharing or charge transfer from the inhibitor molecule to the metal surface resulting in the formation of coordinative type bond. This is in fact possible in view of the presence of unshared electron pairs in the organic compounds molecules and taking into a consideration the behavior of ferrous metal as electrons acceptor because of its incomplete d-submonolayer.

The investigated inhibitors block significantly some of the active sites on the metal surface inhomogeneous energetically. In general, the inhibitors adsorb at the most active sites of the surface with lowest E_a and thus isolate them. Other active sites of higher E_a take part in the further corrosion process. Their number is much greater as the value of A in the presence of inhibitor is higher (E_a (inh) > E_a (1M HCl)). Indeed, A is connected with active sites number in a heterogeneous reaction. When E_a (inh) < E_a (1M HCl); i.e. in the presence of the studied inhibitors, then the value of A is less than that in 1 M HCl. This means that the adsorption of the inhibitor results in less in number but more active (with lower E_a) sites which participate in the further corrosion process and determine its apparent activation energy. Hence a partial compensation effect can be observed [14,41]. Similar results were obtained with quaternary ammonium bromides of N-containing heterocyclic in both HCl and H_2SO_4 acids as reported by Popova et al. [42]

Furthermore, an alternative formulation of Arrhenius equation is (15) [43]:

$$\ln \frac{i_{corr}}{T} = \left(\ln\left(\frac{R}{Nh} \right) + \frac{\Delta_a S^*}{R} \right) - \frac{\Delta_a H^*}{RT} \qquad (15)$$

Where h is Plank's constant, N is Avogadro's number, $\Delta_a S^*$ is the entropy of activation and $\Delta_a H^*$ is the enthalpy of activation.

Fig. 7 shows the plot of $ln\ i_{corr}/T$ vs. $1/T$ for the blank and the studied inhibitors at 10^{-3} M. Straight lines are obtained with a slope of $(-\Delta_a H^*/R)$ and an intercept of $(lnR/Nh + \Delta_a S^*/R)$ from which the values of $\Delta_a H^*$ and $\Delta_a S^*$ are calculated and are listed in Table 5. The positive sign of the enthalpies $\Delta_a H^*$ reflects the endothermic nature of the steel dissolution process whereas large negative values of entropies $\Delta_a S^*$ imply that the activated complex in the rate determining step represents an association rather than a dissociation step, meaning that a decrease in disordering takes place on going from reactants to the activated complex [44-46].

3.5. Effect of immersion time on corrosion inhibition

Figure 9 represents the impedance diagrams in the Nyquist representation recorded for the mild steel in 1M HCl with 10^{-3} M of the studied inhibitors in order to assure that the achieved coverage degree is close to the maximal value.

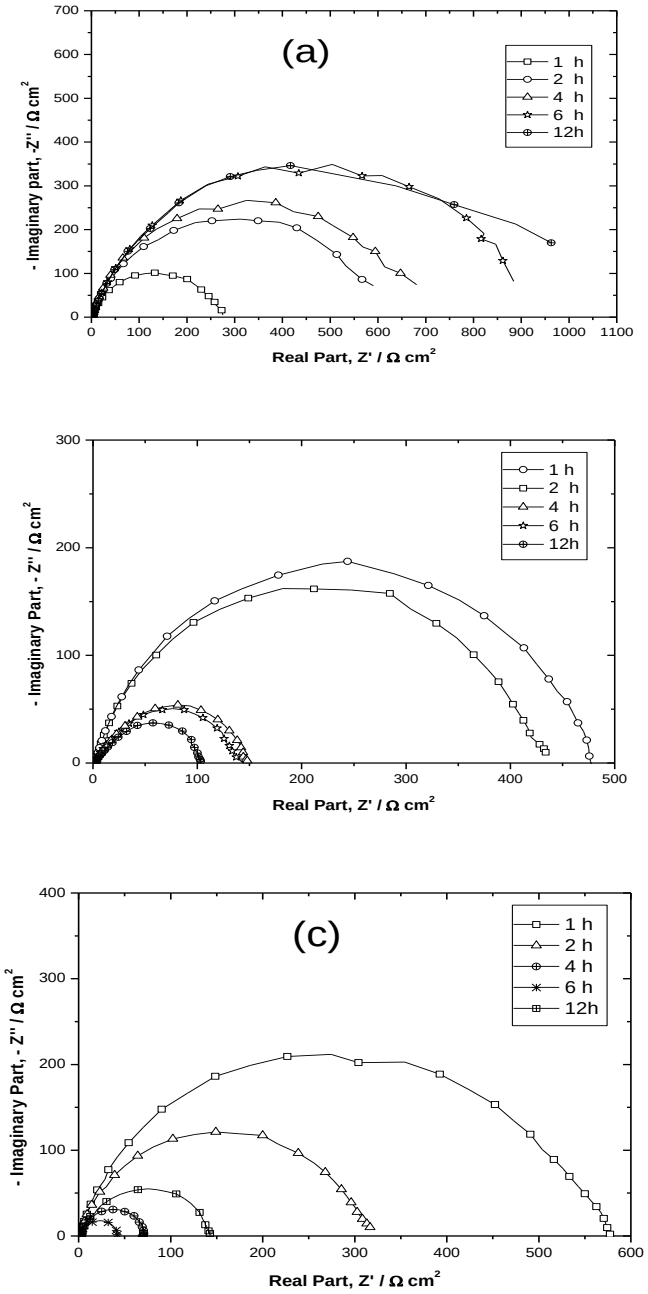

Figure 9. Effect of immersion time on the behaviour of the mild steel/1M HCl interface in the presence of 10^{-3} M of (a) *IND*, (b) *IND-TET* and (c) *TET*

The EIS response of the mild steel is one depressed semicircle. In this case, the semicircular shape is indicative of the charge transfer resistance R_{ct} in parallel with a constant phase element *CPE* of the metal/solution interface, and connected in series with solution resistance R_{Ω} as shown in Fig. 4. Consequently, the equivalent circuit described in Fig. 4 is used to fit the experimental results and to obtain the different corrosion parameters.

The relations between the immersion time and both of R_{ct} and C_{dl} are given in Fig. 10 (a) and (b), respectively. It is appears clearly from these figures that in the case of *IND*, the total impedance of

the system increases rapidly from 1h to 12h – an opposite behavior is observed with *IND-TET* and *TET* for which a decrease in the transfer resistance is registered. It is to be noted for *IND-TET* that the decrease is registered in the first stage till 4h and remained fairly constant afterward.

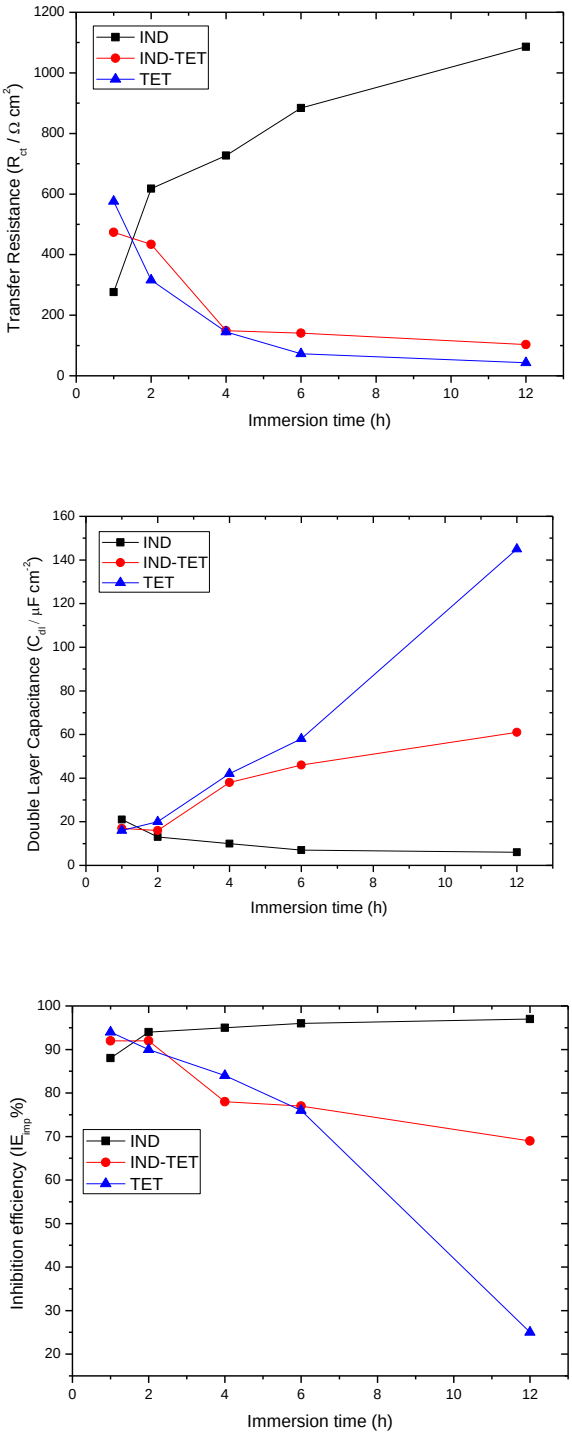

Figure 10. EIS parameters obtained under open circuit conditions at different immersion times: system mild steel / 1 M HCl added of 10^{-3} M of the studied inhibitors at 298 K

At the same time, the values of C_{dl} were increased rapidly at the earlier times of immersion in the case of *IND-TET* and *TET* and subsequently in the case of *TET*, whereas a slightly decrease is observed with *IND*. Note that all values of charge transfer and double layer capacitance are higher in the free 1M HCl medium (not shown here) over all the studied period of time as a result of the formation of inhibitors surface films.

The inhibition efficiency, $IE_{imp}\%$, of the investigated inhibitors was derived from the R_{ct} values at different immersion times using equation (4). It is clear from Fig. 10 (c) that $IE_{imp}\%$ increases during the initial 2 h and remained fairly constant afterward for *IND* inhibitor.

These results demonstrate that the formation of surface film, and therefore the *IND* adsorption, on the electrode surface is reinforced with immersion time and is relatively fast and completed within ca. two hours. Similar result was recently observed in a previous paper [47].

However, in the case of *IND-TET*, for longer times, $IE\%_{imp}$ decreases and subsists at reasonable values at least till 6 h and slows down to attain 69% at 12 h of immersion. Moreover, *TET*, $IE\%_{imp}$ drops dramatically with immersion time. It reaches only 25% after 12 h in 1 M HCl added with 10^{-3} M of *TET*. The corrosion rate is higher in the longer times that in the first stage of immersion, perhaps because the formed film is not stable as a function of time. Sometimes some inhibitors show a very good behavior during short times but not in long periods. In long term test *IND-TET* and essentially *TET* do not keep their protective characteristics. Obviously the protective layer is not stable and it seems that a soluble complex with mild steel forms. Thus the decrease of $IE\%_{imp}$ maybe attributed to the induction of the corrosion process as a result of permeation of the electrolyte through the inhibitor protection layer. Similar results were reported by other coworkers [48].

4. CONCLUSION

1. Reasonably good agreement was observed between the data obtained from potentiodynamic polarization and electrochemical impedance spectroscopy techniques.

2. *IND* and *IND-TET* slow down the cathodic reaction then considered as cathodic type inhibitors whereas *TET* slows down the cathodic reaction to greater extents than the anodic one which suggests that *TET* mainly acts as mixed-type inhibitor.

3. The adsorption of all inhibitors is well described by the Langmuir adsorption isotherm. All values of the standard Gibbs energy of adsorption are negative and less in absolute values $|\Delta_{ads}G°|$ than 40 kJ mol^{-1}. These results confirm that both of chemisorption and physisorption control the adsorption phenomenon.

4. $IE_{I\text{-}E}\%$ of the studied inhibitors was circa temperature-independent which means that all compounds maintain and even increase their protective effect at higher temperatures. The lower values of the apparent activation energy in inhibited media are related to lower values of the pre-exponential factors, showing compensation effect. Very good inhibition efficiency was observed with *TET* at 55°C; >97%. These results reveal the nature character of adsorption which seems to be only chemisorption.

5. $IE_{imp}\%$ of the studied inhibitors was time-dependent. The inhibition efficiency increases with time in the case of *IND* and an opposite trend is observed in the case of *IND-TET* and *TET*. These

results reveal the chemisorption character for *IND* and the physisorption one for the others. Very good inhibition efficiency was observed with *IND* after 12 h; >96% and very bad one was registered with *TET*; <25%.

6. The impact of concentration, temperature and immersion time taken together on corrosion inhibition process demonstrates the double character nature of the adsorption phenomena. It remains not evident to attribute bluntly either chemisorption or physisorption mechanism for the studied inhibitors. The authors believe that the studied inhibitors are adsorbed by mixed mode (physisorption and chemisorption both involved to some extent) onto the mild steel interface.

References

1. G. Schmitt, *Br. Corros. J*. 19 (1984) 165.
2. G. Trabanelli, in: F. Mansfeld (Ed.), Corrosion Mechanism, Marcel Dekker, New York, 1987.
3. Zarrouk, B. Hammouti, H. Zarrok, M. Bouachrine, K.F. Khaled, S.S. Al-Deyab, *Int. J. Electrochem. Sci.*, 7 (2012) 89.
4. W. Li, Q. He, C. Pei,B. Hou, *Electrochim Acta* 52 (2007) 6386.
5. B. Zerga, A. Attayibat, M. Sfaira, M. Taleb, B. Hammouti, M. Ebn Touhami, S. Radi, Z. Rais, *J. Appl. Electrochem*. 40 (2010) 1575.
6. M. Scendo, M. Hepel, *Corros. Sci*. 49 (2007) 3381.
7. A.Dafali, B. Hammouti, A. Aouniti, R. Mokhlisse, S. Kertit, K. Elkacemi, *Ann. chim. Sci. Mat*., 25 N°3 (2000) 437
8. L. Larabi, O. Benali, S.M. Mekelleche, Y. Harek, *Appl. Surf. Sci*. 253 (2006) 1371.
9. B. Zerga, R. Saddik, B. Hammouti, M. Taleb, M. Sfaira, M. Ebn Touhami, S.S. Al-Deyab, N. Benchat, *Int. J. Electrochem. Sci*., 7 (2012) 631.
10. B. Zerga, B. Hammouti, M. Ebn Touhami, R. Touir, M. Taleb, M. Sfaira, M. Bennajeh, I. Forsal, *Int. J. Electrochem. Sci*., 7 (2012) 471.
11. M. Mihit, R. Salghi, S. El Issami, L. Bazzi, B. Hammouti, El. Ait Addi, S. Kertit, *Pigm. Resin Technol.* 35 (2006) 151
12. M. Mihit, S. El Issami, M. Bouklah, L. Bazzi, B. Hammouti, E. Ait Addi, R. Salghi, S. Kertit, *Appl. Surf. Sci*. 252 (2006) 2389.
13. N.O. Eddy, B.I. Ita, N.E. Ibisi, Ebenso, *Int. J. Electrochem. Sci*., 6 (2011) 1027.
14. A.Popova, *Corros. Sci*. 49 (2007) 2144.
15. A.Boukamp, *Users Manual Equivalent Circuit, ver*. 4.51 (1993).
16. M.S. Abdel Aal, S. Radwan, A. El Saied, *Br. Corros. J*. 18 (1983) 2.
17. K.F. Khaled, M.M. Al-Qahtani, *Mater. Chem. Phys*. 113 (2009) 150.
18. W.R. Fawcett, Z. Kovacova, A. Motheo, C. Foss, J. Electroanal. Chem. 326 (1992) 91.
19. F. Mansfeld, *Corrosion* 36 (1981) 301.
20. J.R. Macdonald, *J. Electroanal. Chem*. 223 (1987) 25.
21. S. Duval, M. Keddam, M. Sfaira, A. Srhiri, H. Takenouti, *J. Electrochem. Soc*. 149 (2002) B520.
22. J. Pang, A. Briceno, S. Chander, *J. Electrochem. Soc*. 137 (1990) 3447.
23. S.F. Mertens, C. Xhoffer, B.C. De Cooman, E. Temmerman, *Corrosion* 53 (1997) 381.
24. M. Lagrenée, B. Mernari, M. Bouanis, M. Taisnel, F. Bentiss, *Corros. Sci*. 44 (2002) 573.
25. A.Srhiri, M. Etman, F. Dabosi, *Werkst. Korros*. 43 (1992) 406.
26. K.S. Khairou, A. El-Sayed, *J. Appl. Polym. Sci*. 88 (2003) 866.
27. C.H. Hsu, F. Mansfeld, *Corrosion* 57 (2001) 747.

28. V Ramesh Saliyan and Airody Vasudeva Adhikari, *Bull. Mater. Sci*. 31 (2008) 699.
29. F. Bentiss, M. Lebrini, M. Lagrenée, M. Traisnel, A. Elfarouk, H. Vezin, *Electrochim. Acta* 52 (2007) 6865.
30. E. Khamis, F. Bellucci, R.M. Latanision, E.S.H. El-Ashry, *Corrosion* 47 (1991) 677.
31. H. Ashassi-Sorkhabi, B. Shaabani, D. Seifzadeh, *Appl. Surf. Sci*. 239 (2005) 154.
32. I.A. Ammar, F.M. El Khorafi, *Werkst. Korros*. 24 (1973) 702.
33. E.S. Ivanov, Inhibitors for Metal Corrosion in Acid Media, Metallurgy, Moscow, 1986.
34. L.N. Putilova, S.A. Balesin, V.P. Barranik, Metallic Corrosion Inhibitors, Pergamon Press, New York, 1960.
35. N.P. Zhuk, Course on Corrosion and Metal Protection, Metallurgy, Moscow, 1976.
36. T. Szauer, A. Brandt, *Electrochim. Acta* 26 (1981) 1209.
37. F. Bentiss, M. Traisnel, L. Genegembre, M. Lagrenée, *Appl. Surf. Sci*. 152 (1999) 237.
38. A.Popova, E. Sokolova, S. Raicheva, M. Christov, *Corros. Sci*. 45 (2003) 33.
39. B. Mernari, L. Elkadi, S. Kertit, *Bull. Electrochem*. 17 (2001) 115.
40. R. Raicheff, K. Valcheva, E. Lazarova, in: Proceeding of the Seventh European Symposium on Corrosion Inhibitors, Ferrara, Italy, 1990, p. 48.
41. A.Popova, M. Christov, A. Vasilev, *Corros. Sci*. 49 (2007) 3276.
42. J.O M. Bochris, A.K.N. Reddy, Modern Electrochemistry, vol. 2, Plenum Press, New York, 1977, p. 1267.
43. J. Marsh, Advanced Organic Chemistry, third ed., Wiley Eastern, New Delhi, 1988.
44. S. Martinez, I. Stern, *Appl. Surf. Sci.* 199 (2002) 83.
45. M. Dahmani, A. Et-Touhami, S.S. Al-Deyab , B. Hammouti, A. Bouyanzer, Corrosion inhibition of C38 steel in 1 M HCl Int. *J. Electrochem. Sci.,* 5 (2010) 1060.
46. S. Aloui, I. Forsal, M. Sfaira, M. Ebn Touhami, M. Taleb, M. Filali Baba, M. Daoudi, *Portugaliae Electrochimica Acta* 27 (2009) 599.
47. F. Zucchi, G. Trabanelli, M. Fonsati, *Corros. Sci*. 38 (1996) 2019.